Thermal measurements used to characterize the fatigue properties of elastomeric materials at micro scales

I. Masquelier [1], Y. Marco[1], V. Le Saux[1], C. Doudard[1], S. Calloch[1], P. Charrier[2]

[1] ENSTA Bretagne – Laboratoire Brestois de Mécanique et des Systèmes, 2 rue François Verny, 29806 Brest Cedex 08
isaure.masquelier@ensta-bretagne.fr, yann.marco@ensta-bretagne.fr, vincent.le-saux@ensta-bretagne.fr
[2] Trelleborgvibracoustics, Z.I. Nantes Carquefou, BP10419, 44474 Carquefou Cedex
pierre.charrier@tbvc.com

ABSTRACT
The fatigue properties of elastomeric materials highly depend on their microstructure. At a macro-scale, energy based criteria has proven to be efficient, but the understanding of the link to the microstructure is very difficult because of the numerous dissipation sources involved. The aim is here to understand what happens around a few inclusions and within a limited number of cycles (up to 2000), thanks to thermomechanical measurements at this scale. Reaching high enough spatial and thermal resolutions are therefore the two main difficulties encountered. As a first step, protocol and characterization tools of the thermal gradients has been developed on samples with geometric heterogeneities (hole or crack) and then applied on bad mixed samples (sample where inclusions are bigger than normally). Both loading cases at the macro and micro scales imply multiaxial mechanical conditions. The experimental fields of dissipated energy are finally compared to the ones obtained from numerical simulations.

INTRODUCTION

Several criterions for fatigue have been developed, nevertheless they remain macroscopic and a recent review underlined that the microstructure is not really accounted for [1]. In a recent paper, based on thermal measurements and micro-tomography measurements, an energetic criterion [2] opens the way to integrate the influence of the microstructure. Bridging the dissipated energy observed at a macroscopic scale to the energy dissipated by the basic fatigue mechanisms nevertheless clearly remains a difficult challenge. The aim of this study is to improve the description of the dissipated energy at low scales thanks to temperature measurements. This requires a specific experimental set up and a dedicated protocol to characterize the local dissipation gradients that are firstly developed on samples with a geometric heterogeneity before being applied on badly dispersed mixes.

1. EXPERIMENTAL SETTINGS

1.1.Material and samples

This study is realized with a synthetic rubber filled with carbon blacks, classically used for automotive components. Table 1 gives some information on the material recipe.

Table 1 : Rubber compounding (phr: per hundred rubber)

Component	Content (phr)
SBR 1723	137.5
N550	43
Zinc oxide	5
Stearic acid	2
Nytex 820	3
Sulphur (80%)	2.25
CBS (80%)	3.125
IPPD	1
TMQ	1

The experiments are achieved on very thin samples (0.2mm) that help reducing the identification of the thermal sources to a two dimensions problem. The dimensions of the sample are given on Figure 1.

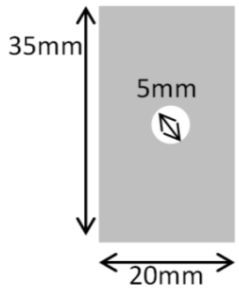

Figure 1 : Geometry of the sample

Thin particles are painted on the sample and are used as thermal markers. The kinematic filed are then obtained by image correlation, based on the infrared images [3].

1.2.Experimental devices

All tests are achieved on a Bose electrodynamical testing machine equipped with a 3.2kN cell force and are displacement controlled. The thermal acquisition is performed thanks to a FLIR SC7600-BB infrared camera with two objective lenses available, one

of 50mm, and one called “G1”, which means that the size of the zone observed is the same as the size of the detector (7mm*5mm). To improve the thermal resolution an individual pixel (ie pixel-wise) calibration taking into account the influence of the internal camera temperature is used, as well as a bad pixel correction. After this specific calibration, a precision of 10mK is obtained for differential measurements.

1.3.Measurement protocol

The sample is submitted to a sinusoidal signal between 0 and 12mm at 10Hz during 700 cycles, and then it is kept at the maximal deformation for 120s during the cooling. All along the experiment, a desynchronized thermal acquisition is performed at 9.7Hz (Figure 2). These loading conditions insures to get a high enough thermal signal and to reach a stabilized mean temperature before the cooling step. The cooling is performed at the maximal deformation to avoid a possible bucking induced by the geometry of the sample and its major goal is to identify the kinetic of the thermal equilibrium recovery. A cardboard box and a sheet are also used to limit the influence of the environment.

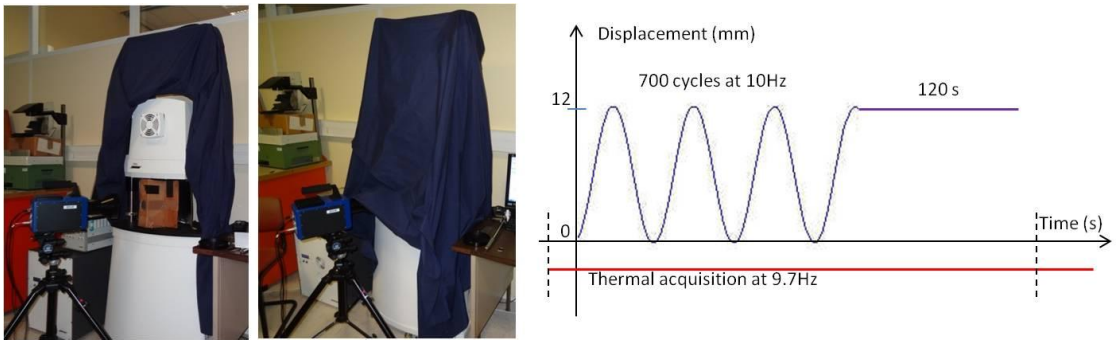

Figure 2 : Experimental devices and mechanical protocol

2. ANALYSIS PROTOCOLS

In order to trace back the source terms, several analysis protocols based on the heat equation are developed [4].

$$\rho C_p \dot{T} - \lambda \Delta T = \Delta + r + C_T + C_E \quad (1)$$

Where ρ is the density, C_p the specific heat, T the temperature, λ the thermal diffusion coefficient, Δ the intrinsic dissipation, r the internal heat production, C_T the couplings with temperature of the internal variables and C_E the thermo-elastic couplings. In our study, there is no internal heat production and the couplings with temperature are negligible. Equation 1 becomes:

$$\rho C_p \dot{T} - \lambda \Delta T = \Delta + C_E \quad (2)$$

2.1.Temperature mappings

A first possibility to identify the heat source field is to analyse the temperature field obtained from infrared images. As the temperature variation is not intrinsic to the material, a thermomechanical modelling is needed. Then the reconstruction of the heat source mapping is performed by solving the heat equation via an inverse analysis [5]. With elastomeric materials there are several additional difficulties: the high strains framework, the low thermal conductivity, the lack of efficient thermomechanical modelling accounting for dissipation sources and also the fact that the emissivity depends on the temperature that can generate some artefacts. In the study presented here, an experimental approach is suggested.

2.2.Source terms mappings

A second possibility developed by M. Poncelet [6] is to subtract two images. The first one measured during the loading step when the source terms are active, the other one during the cooling when the source terms are inactive. The image of the cooling is chosen so that the mean temperature of the second image is the same as the first one. This permits to minimize the possible artefacts induced by the dependence of the emissivity on temperature (Figure 3).

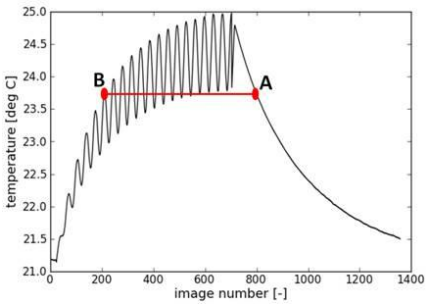

During the cycling, source terms are active, image (B):

$$\rho\, C_p\, \dot{T}_B - \lambda \Delta T_B = \Delta + C$$

During the cooling, source terms are inactive, image (A):

$$\rho\, C_p\, \dot{T}_A - \lambda \Delta T_A = 0$$

Figure 3 : Protocol for source terms mapping

This protocol was developed for metallic materials and leads to trace back the source terms subject whatever the mean temperature. Applied to elastomeric materials, the maps of dissipated energy can be obtained (Figure 4) but the low thermal conductivity of these materials limits the spatial description of the gradients. The result obtained from the subtraction of images A and B therefore depends on the chosen mean temperature (Figure 5).

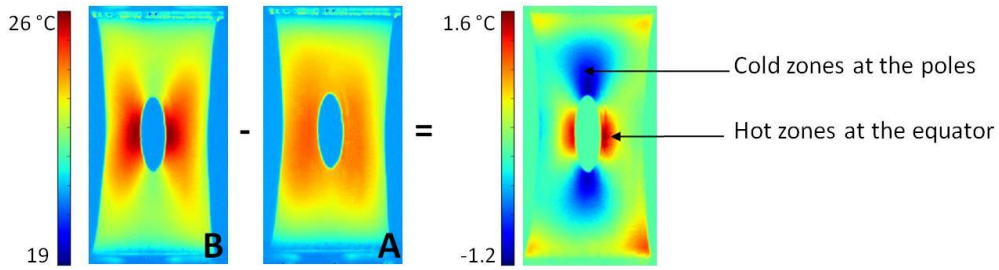

Figure 4 : Example of source terms mapping

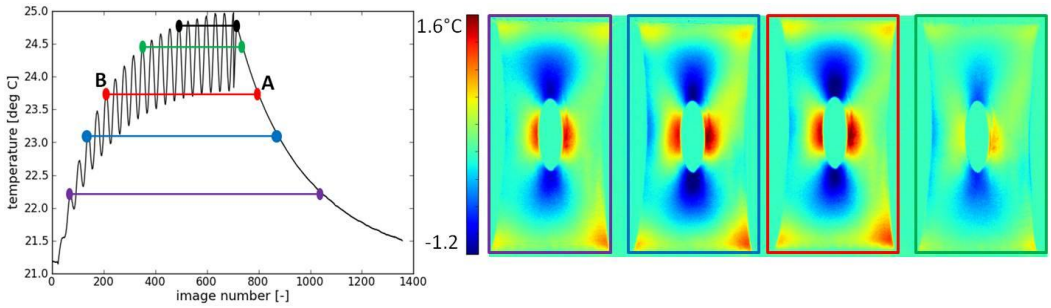

Figure 5 : Example for gradient loss because of the diffusion

2.3.Dissipation mappings

In order to neglect the diffusion, a solution is to consider two very close instants at the beginning of the cyclic loading [7] (Figure 6). In fact, the characteristic time of the thermal equilibrium of our sample is about 40s; it takes into account the loss by diffusion and by exchange with the environment. In our study, there is 3.6s between two successive identical mechanical states, so we consider that the heat diffusion and loss are negligible for the two first states. We directly obtain a mapping of the intrinsic dissipation (Figure 7), in fact the heat equation becomes:

$$\rho\, C_p\, \dot{\theta} = \Delta \tag{3}$$

Where $\dot{\theta} = \frac{(T_B - T_A)}{t_B - t_A}$

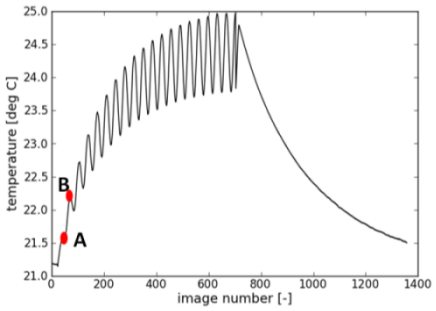

Figure 6 : Protocol for dissipation mapping

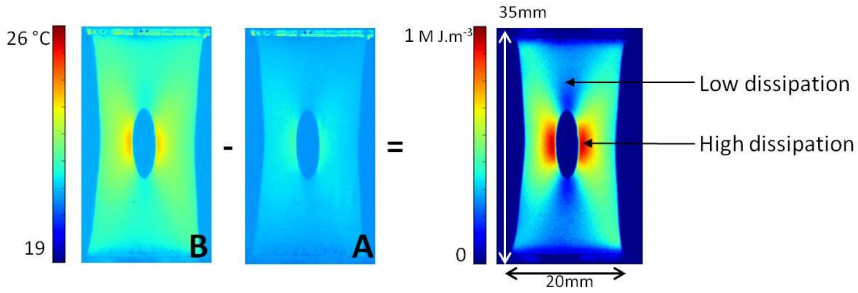

Figure 7 : Example of dissipation mapping

Finally, this protocol provides good spatial and thermal resolutions. Furthermore, considering the same mechanical configurations for two close times, it enables to neglect the diffusion, to split the intrinsic dissipation from the thermo-elastic couplings and to limit the artefacts due to the emissivity.

2.4.Validation at a lower scale

The latter protocol is applied on a thin sample with a lateral crack and then on bad mixed sample (Figure 8). It should be noted that the mean values used for the density ρ and the specific heat C_p can be questioned, at this microscopic scale.

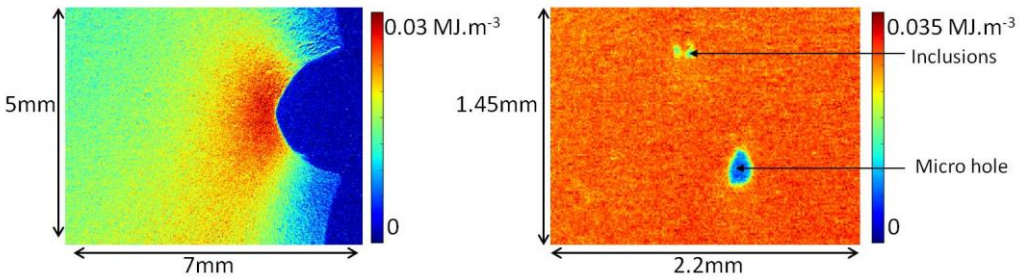

Figure 8 : Dissipation mappings of cracked and bad mixed samples

3. KINEMATIC MEASUREMENTS & COMPARISON TO A MODEL

In order to compare the energy fields obtained from tests to the simulated ones, the knowledge of the local strain fields is mandatory. The choice is here to use the thermal data to perform the measurement of the kinematic fields. The interest is obviously to characterize in one measurement the temperature fields and the displacement fields. A monotonic tension is performed between 0 and 12mm at a speed of 0.5mm/s and a thermal acquisition is realized at 10Hz during the loading. The displacement and strain fields are obtained thank to image correlation performed with Correli® and are compared with the results of finite elements simulations (Figure 9).

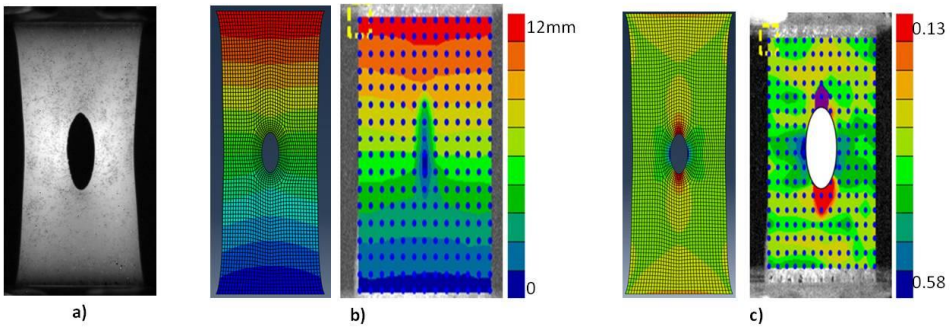

Figure 9: a) Infrared image – b) Displacement fields - c) Logarithmic strain fields

The finite elements simulation is done using the Abaqus® software, with a 3D modelling with only one element in the thickness. We use hybrid and linear elements (C3D8H) and a Mooney-Rivlin hyperelastic potential. Then, a computation is performed with the energetic modelling developed by Y. Le Chenadec [8], which allows for obtaining the dissipated energy from the cyclic hyperelastic energy:

$$E_{diss} = \kappa E_{cycl}^{\gamma} \tag{5}$$

Where E_{diss} is the dissipated energy, E_{cyc} the cyclic energy such as:

$$E_{cyc} = \int_{E_{min}^{(0)}}^{E_{max}^{(0)}} \left(T^{(0)} - T_{min}^{(0)}\right) : dE^{(0)} \tag{6}$$

Where $E^{(0)} = \ln U$ and $T^{(0)} = JR^t \sigma R$ are the order 0 combined Hill tensors.

The parameters κ and ɣ are two constants that depend on the material. They are identified on hourglass shaped samples with the method proposed by Le Saux et al [9]. We observe a pretty good correlation between the energy fields measured and predicted (Figure 10) that opens the way to lowest scales.

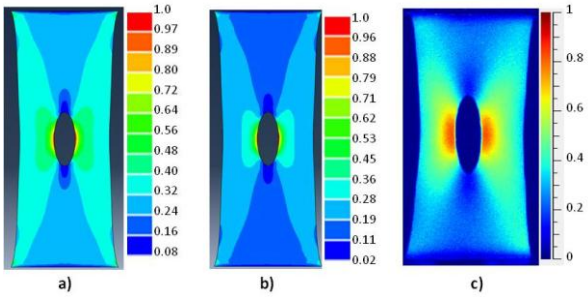

Figure 10: a) Principal maximal strain [100%] – b) Dissipated energy [MJ.m^{-3}] obtained by simulation – c) Intrinsic dissipation [MJ.m^{-3}] obtained experimentally

CONCLUSION

The proposed analysis protocol leads to have different information with only one measurement: a 2D kinematic field and an experimental mapping of the intrinsic dissipation. The thermal resolution seems to be relevant to characterize the fatigue basic mechanisms at the microscopic scale.

ACKNOLEDGEMENT

The authors would like to thank the ANR for its financial support (ANR–2010–RMNP-010-01) and all the partners of the PROFEM project, TBVC, GeM, UBS and LRCCP. A special thank to Chloé Marco for her sequins pen.

REFERENCES

1. Mars W., Fatemi A., (2002) International Journal of Fatigue, **24**, 949-961.
2. Le Saux V., Marco Y., et al. (2010), International Journal of Fatigue, **32,** 1582-1590.
3. Maynadier A., Poncelet M. et al. (2010), Experimental Mechanics, **52**, 241-255.
4. Lemaître et Chaboche, 2004, Mécanique des matériaux solides, Dunod.
5. Doudard C., Calloch S. et al (2010), Mechanics of Materials, **42**, 55-62.
6. Poncelet M. (2007) Thesis, Ecole Normale Supérieure de Cachan, France.
7. La Rosa G., Risitano A., (2000), International Journal of Fatigue, **22**, 65-73.
8. Le Chenadec Y., (2007) ECCMR.
9. Le Saux V., Marco Y., et al. (2012) Rubber Chemistry and Technology, in press.